

# Rail wear rate on the Belgian railway network – a big-data analysis

Tim Vernailen, Li Wang, Alfredo Núñez, Rolf Dollevoet & Zili Li

**To cite this article:** Tim Vernailen, Li Wang, Alfredo Núñez, Rolf Dollevoet & Zili Li (30 Sep 2023): Rail wear rate on the Belgian railway network – a big-data analysis, International Journal of Rail Transportation, DOI: [10.1080/23248378.2023.2259392](https://doi.org/10.1080/23248378.2023.2259392)

**To link to this article:** <https://doi.org/10.1080/23248378.2023.2259392>



© 2023 The Author(s). Published by Informa UK Limited, trading as Taylor & Francis Group.



Published online: 30 Sep 2023.



Submit your article to this journal [↗](#)



Article views: 501




View related articles [↗](#)



View Crossmark data [↗](#)

# Rail wear rate on the Belgian railway network – a big-data analysis

Tim Vernailen<sup>a,b</sup>, Li Wang <sup>a</sup>, Alfredo Núñez<sup>a</sup>, Rolf Dollevoet<sup>a</sup> and Zili Li<sup>a</sup>

<sup>a</sup>Section of Railway Engineering, Delft University of Technology, Delft, The Netherlands; <sup>b</sup>Department of Civil Engineering - Track Maintenance, Infrabel, Brussels, Belgium

## ABSTRACT

This paper presents a big data-based analysis of the rail wear of the whole Belgian railway network measured in 2012 and 2019. Wear rates are reported, discussed, and quantitatively formulated as functions of critical factors in terms of curve radius, annual tonnage (rail age), high rail in curves, an average from both rails in straight tracks at rail top (vertical wear) and gauge corner (45° wear) and for steel grade R200 and R260. The influence of preventive grinding is also analysed. The wear rates are derived in an aggregated manner for the whole network. The wear rates do not show significant change with changes in rolling stock over the years, implying that the wear rates could also hold for other networks. It is found that R200 shows, on average, a 34% higher wear rate than R260. Also, the wear rate per tonnage is lower for high-loaded tracks. Thus, time is a relevant factor in explaining the wear evolution of low-loaded tracks; for instance, the effect of corrosion may have an important role. The paper provides statistically significant information that can be used for wear modelling, understanding and treating rolling contact fatigue based on the wear rate and developing tailored rail maintenance strategies.

## ARTICLE HISTORY

Received 17 May 2023

Revised 16 August 2023

Accepted 11 September 2023

## KEYWORDS

Rail; wear rate; big data; country-wide assessment

## 1. Introduction

An important challenge for railway infra managers is to avoid or minimize the changes in rail and wheel contact surfaces due to wear [1]. New technologies and methods to control wear are needed to maintain train stability and passenger comfort, decrease rail and track system degradation and reduce the risk of derailment. Rail wear is a complex phenomenon that depends on the local conditions of the infrastructure, the rolling stock, and the exogenous variables such as the environment and weather conditions at the track location. Rail wear varies by location because of the many stochasticities in the involved parameters that can change with time and space [2]. Wear is usually assumed to be proportional to frictional work [3]. The proportionality and frictional work are functions of the rail steel grade (such as R260 and R200), wheel steel grade (such as ER6 and ER7), pairing between rail material and wheel material, normal contact stress, coefficient of friction, and relative slip [4]. Rail wear is also influenced by the design, construction, and maintenance of the vehicles (primary yaw stiffness, braking and traction control, etc.), tracks (radii of curves, cant, etc.), the rail and wheel profiles, the surface treatments such as coating or lubrication, the interaction between the vehicles and the tracks, and the environment (humidity, corrosion, etc.) [5,6]. A discussion of the influence of some of the design parameters for certain material pairings is given in [1].

**CONTACT** Alfredo Núñez  A.A.NunezVicencio@tudelft.nl  Section of Railway Engineering, Delft University of Technology, Stevinweg 1, Delft 2628CN, The Netherlands

© 2023 The Author(s). Published by Informa UK Limited, trading as Taylor & Francis Group.

This is an Open Access article distributed under the terms of the Creative Commons Attribution-NonCommercial-NoDerivatives License (<http://creativecommons.org/licenses/by-nc-nd/4.0/>), which permits non-commercial re-use, distribution, and reproduction in any medium, provided the original work is properly cited, and is not altered, transformed, or built upon in any way. The terms on which this article has been published allow the posting of the Accepted Manuscript in a repository by the author(s) or with their consent.

The many influencing parameters and uncertainties hinder deriving simple mathematical laws for wear behaviour. Wear mapping of materials is a common research practice [7]. Various assumptions are usually considered when determining the wear behaviour in laboratories. In [8], the relations between rail wear rate regimes and transitions obtained from twin disc tests, pin-on-disc machines, and field measurements are discussed. The normal stress and relative slip can be controlled in a laboratory environment and small-scale field tests [9]. Managing the relative slip becomes difficult for large-scale field operational conditions. Although many small-scale field data are available for standard rail grades, a systematic analysis of rail wear over a long period and on a country-wide network is rare [8,10]. Numerical models are also essential for exploring wheel and rail wear. Many numerical models have been developed, and the modelling strategy varies from a single wear calculation to iteration of dynamic simulations [11–14]. In practice, rail wear and rolling contact fatigue (RCF) develop simultaneously. The competitive effects between wear and RCF should be treated carefully in the simulations [15,16].

This paper analyzes the wear behaviour of rails from long-term monitoring measurements of the whole Belgian railway network. The wear rates are derived and analysed based on the rail steel grades, the curve radius, the UIC classes of annual traffic load, and the accumulated million gross tons (MGT). Wear data from two measuring campaigns, conducted in 2012 on 4,409 km tracks and in 2019 on 5,338 km tracks, are analysed.

The paper is organized as follows. In [Section 2](#), the wear measurement data is described. [Section 3](#) analyzes the data and presents the results and discussions. [Section 4](#) shows conclusions and further research.

## 2. Rail wear measurement

### 2.1. Description of the Belgian network and parameters to be analysed

Since the late 1990s, the Belgian railway infrastructure manager Infrabel has been using an automatic train-borne measuring system to monitor the rail parameters mounted on the EM130 measurement train. The recorded rail parameters include vertical wear, horizontal wear, wear at 45° and inclination of the rails. The railway network is typically divided into homogenous sections of 50 m for analysis. A requirement for a track section to be homogenous is that the rails (age, profile, and steel grade) and annual train tonnage are the same. The measurements are matched with a technical inventory that includes the detailed status of the track asset, which the local track managers constantly update. All relevant data are then averaged in each of the 50 m sections following the technical inventory.

By 2020, the Belgian railway network consisted of 422 km of high-speed lines, 222 km of freight lines, and 5,853 km of conventional lines with mixed passenger and freight traffic. In this paper, only the conventional lines with mixed passenger and freight traffic are considered. The rails are installed with an inward inclination of 1:20. The nominal gauge is 1435 mm, and two rail profiles are used in the plain track: the UIC60E1 profile and the Belgian 50E2 profile [17]. These two profiles have different geometrical dimensions, but the widths of the railhead and the profiles are equal. The most commonly utilized rail materials are pearlitic steels. In 1982, Infrabel started replacing steel grade 700 (chemical composition, % by mass: C 0.4/0.6, Si 0.05/0.35, Mn 0.8/1.25 and RM 680/830MPa) according to UIC leaflet 860–0 with R260 (EN13674–1) steel grade (chemical composition, % by mass: C 0.62/0.8, Si 0.15/0.58, Mn 0.7/1.20 and RM ≥ 880MPa). The steel grade 700 (UIC 860–0) is referred in the rest of the document as R200 (EN13674–1) because the chemical composition is closest (chemical composition, % by mass: C 0.4/0.6, Si 0.15/0.58, Mn 0.7/1.20 and RM ≥ 680MPa). This steel grade corresponded no longer to the needs in track, due to its greater sensitivity to wear. Both steel grades R200 and R260 are not heat treated. Over the years, the steel manufacturing process has been improved, reducing the occurrence of internal defects. However, regarding surface defects, experiences on the Belgian and French railway networks indicate that these changes decreased the wear but might trigger more surface defects. Approximately 66%, 32% and 2% of the network consist of R260 rails, R200 rails

installed before 1982, and R350 rails or rails with high hardness, respectively. This paper will focus on R200 and R260, as the number of rails of R350 and higher hardness is small.

Wear calculation is influenced by many in-service parameters and production tolerance. The rails used in Belgium conform to the standard EN 13,674–1. The tolerance for the rail height is + 0.5/-1.0 mm for height <165 mm (50E2) and + 0.6/-1.1 mm for height  $\geq$ 165 mm (UIC60E1). This tolerance can influence the calculation of the average wear rate, especially for newly installed rails. Thus, measurements from individual track sections are not applied in this analysis. Individual cases are more sensitive to local variables and manufacturing tolerances. Instead, all measurements for the study are divided into three groups according to the three most significant parameters, i.e., curve radius, rail grade, and load (UIC class), and the analysis is performed on these aggregated data.

## 2.2. Definitions of vertical wear and 45° wear

In this paper, we focus the analysis on vertical wear and 45° wear. Vertical wear is calculated by subtracting the measured rail height from the designed rail height, and the 45° wear is calculated by subtracting the measured length from the reference length of the new profiles at 38 mm below the rail surface on the centre axis of the rail, as illustrated in Figure 1. In tangent tracks, the vertical wear is computed as the average of both rails. In the curves, the high and low rails are separately analysed. On the high rail in curved tracks, wear mainly occurs at the gauge corner, with substantial vertical wear [18]. One of the main types of rolling contact fatigue, head checks, mainly occur in the gauge corner, where 45° wear is measured.

## 2.3. Traffic load

The traffic load is defined in terms of UIC class. In the UIC714R leaflet [19], six groups are defined:

$$UIC_i = \begin{cases} UIC1 & \text{if } 130000[\text{ton/day}] < TL_i \\ UIC2 & \text{if } 80000[\text{ton/day}] < TL_i \leq 130000[\text{ton/day}] \\ UIC3 & \text{if } 40000[\text{ton/day}] < TL_i \leq 80000[\text{ton/day}] \\ UIC4 & \text{if } 20000[\text{ton/day}] < TL_i \leq 40000[\text{ton/day}] \\ UIC5 & \text{if } 5000[\text{ton/day}] < TL_i \leq 20000[\text{ton/day}] \\ UIC6 & \text{if } TL_i \leq 5000[\text{ton/day}] \end{cases} \quad (1)$$

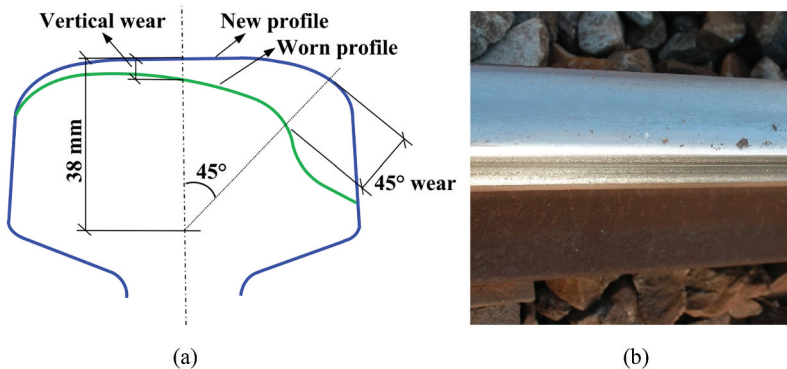


**Figure 1.** Measurements of vertical wear and 45° wear on the railhead (a) definitions of vertical wear and 45° wear (b) typical in situ rail wear.

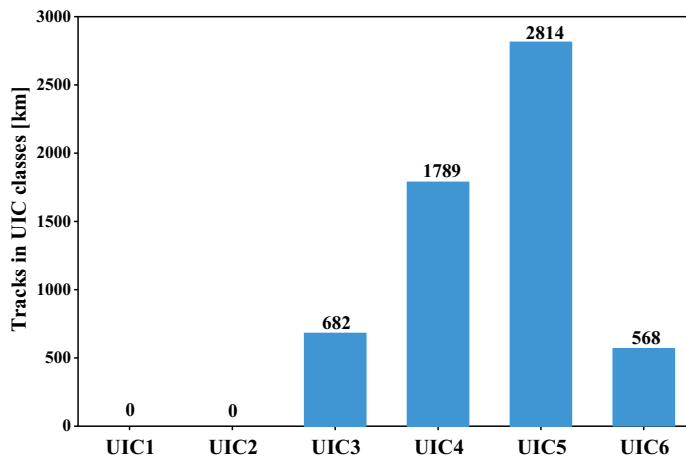


**Figure 2.** Division of the network in UIC classes considered in this paper.

where  $UIC_i$  is the UIC class of track Section  $i$ , and  $TL_i$  is the measured traffic load for track Section  $i$ . All track sections are given a specific UIC class depending on the annual MGT, as shown in Figure 2.

Given the negligible track length in the UIC1 and UIC2 classes, they are not considered in this analysis. The total traffic load in 2011 is used for the wear measurement in 2012 and that in 2018 is employed for the wear measurement in 2019.

#### **2.4. Description of the wear data**

The complete network is measured twice a year with the EM130, and the rail profiles are measured every 25 cm along the track. Wear is recorded as mm/MGT or mm/year. The start time of the wear calculation is the installation date of the rails, and the endpoint of the wear calculation is the moment of measuring the wear.

The measurements for 2012 and 2019 are analysed in this paper. The reason for choosing these two years is that before 2012, negligible preventive grinding was performed. A preventive cyclic grinding programme has been in force since 2012. Thus, in 2019, rail wear consisted of natural wear due to train traffic, as well as corrosion and artificial wear due to grinding. In this paper, wear refers to mechanical wear due to both wheel-rail contact and natural wear due to corrosion unless otherwise indicated. A comparison between the wear measurements in 2012 and 2019 allows the evaluation of the effects of preventive grinding. The Infrabel policy states that grinding is performed at a location only when no rolling contact fatigue (RCF) is reported there. If RCF is reported for a track, that track should not be ground before the rail is replaced. There could, however, be situations where RCF defects were present while the rail was still ground. The data analysis shown indicates that these small inconsistencies between execution and policy do not influence the analysis primarily because the data show good consistency, as will be seen below. The situations of 2012 and 2019 are compared by examining the following data:

- (a) The wear rate derived from the 2012 measurement relative to the dates when the rails were installed.
- (b) The wear rate derived from the 2019 measurement relative to the dates when the rails were installed. The rails considered for the 2019 measurement were installed before and after 2012.

In total, measurements for the 4,409 km and 5,338 km tracks are used for 2012 and 2019, respectively. The complete batch of 5,853 km of tracks is not employed because not all the tracks were measured (due to track works and missing data), and not all the measurements were valid. Data were considered invalid when considerable deviations were observed and extreme values were obtained, e.g.:

- (1) Compared with the nominal rail profile, a recently installed rail will have almost no wear, but it may have a manufacturing deviation of 0.6/-1.1 mm, as illustrated in Figure 3. This deviation can erroneously produce a very high wear rate.
- (2) On some lines, re-used rails were installed. The age of the rail used for the wear calculation is the installation date, but the rail can be many years older, which generates wear rates that are too high.
- (3) The technical inventory was not updated after rail renewal. The measuring system will measure a low wear rate, but the age of the old rail is used for the calculation, which produces very low wear rates.
- (4) The profile recognition system does not always work correctly, e.g., a UIC50E2 profile is taken as UIC60E1. An incorrect profile detection yields extreme values for the wear rate.
- (5) Measurement conditions at different track locations might affect the measurement due to the dynamics of the measurement vehicle, particularly at a point with drastic track geometry changes, such as transitions to bridges and level crossings.

In Figure 4, data of the vertical wear (average of the left and right rails) is shown for the measurements in 2019 for the R260 rail, UIC4 load and tangent tracks. The average vertical wear is 1.20 mm/100 MGT with a standard deviation of 3.50 mm for the complete dataset, i.e., 100% of the data. The data showed extremely high wear rates of up to 60 mm/100 MGT. Such a wear rate is physically impossible and has an important influence on the overall average wear. Thus, data with these large deviations will be removed from the analysis. In Figure 4, the average and standard deviation of the vertical wear are presented when 100%, 95%, 92%, 90% and 85% of the data points are employed for the 5,338 km of tracks in 2019 (0%, 2.5%, 4%, 5% and 7.5% of the data points that are the highest and lowest are removed from the measurements). Based on the 90% dataset, the average vertical wear is 0.82 mm with a standard deviation of 0.62 mm. This 90% dataset will be employed in further analysis, i.e., the 5% highest values and 5% lowest values are not considered in further research.

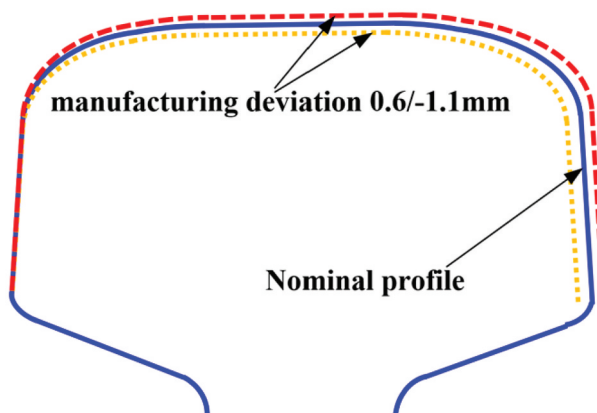


Figure 3. Illustration of manufacturing deviation.

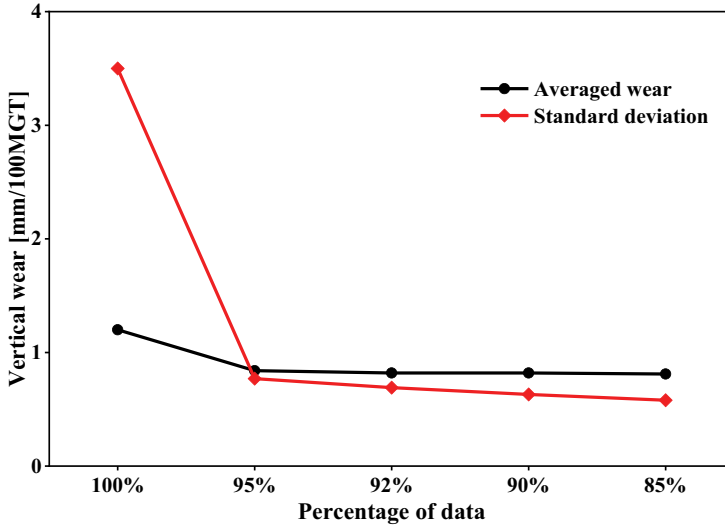


Figure 4. Vertical wear at tangent tracks shows that 5% of the data contains large deviations (2019, R260).

Thus, the analysis will consider the load categories UIC3, UIC4, UIC5 and UIC6. The rail grades are R200 and R260. The curve radius is divided into the following groups:

$$R_i = \begin{cases} 1 & \text{if } R \leq 500[\text{m}] \\ 2 & \text{if } 500[\text{m}] < R \leq 750[\text{m}] \\ 3 & \text{if } 750[\text{m}] < R \leq 1000[\text{m}] \\ 4 & \text{if } 1000[\text{m}] < R \leq 1250[\text{m}] \\ 5 & \text{if } 1250[\text{m}] < R \leq 1500[\text{m}] \\ 6 & \text{if } 1500[\text{m}] < R \leq 2000[\text{m}] \\ 7 & \text{if } 2000[\text{m}] < R \leq 2500[\text{m}] \\ 8 & \text{if } 2500[\text{m}] < R \leq 3000[\text{m}] \\ 9 & \text{if } 3000[\text{m}] < R \end{cases} \quad (2)$$

where  $R_i$  is the number of a curve radius group where track segment  $i$  belongs and  $R$  is the measured radius. Note that tangent tracks are included in the 9<sup>th</sup> group where  $R > 3000[\text{m}]$ . All the measurements are averaged per 50 m and for transition curves also the average curve radius per 50 m is used.

### 3. Data analysis and discussions

#### 3.1. Vertical wear versus tonnage of rails with R260 from measurements in 2012

A railway track consists of tangent and curved parts. The rail will wear differently in these two parts. The rail-wheel contact point is located at the top of the rail in a tangent line, and the vertical wear will thus be the most important. The average vertical wear of both rails is utilized for the analysis of this part. For a curved track, the investigation will be separated for vertical wear and 45° wear at the high rail.

The wear rate is defined as

**Table 1.** Vertical wear (average of both rails) on straight track in relation to UIC class (2012 - R260).

UIC-Class	# km	Vertical wear [mm/100MGT]	Standard deviation [mm/100MGT]
UIC3	700	0.33	0.21
UIC4	809	0.78	0.46
UIC5	564	1.57	1.22
UIC6	67	4.20	3.48
<b>Total</b>	<b>2140</b>	<b>0.93</b>	<b>0.67</b>

$$\Delta w_{vertical}^{traffic} = \frac{w_t}{AL_t(t - t_0)} \times 100 \quad (3)$$

where  $\Delta w_{vertical}^{traffic}$  is the wear rate per 100 MGT in mm/100MGT measured in year  $t$ ,  $w_t$  in mm is the wear measured in year  $t$ ,  $AL_t$  is the annual traffic load in MGT measured in year  $t$ , and  $t_0$  is the year of the rail installation.

Table 1 lists the vertical wear on straight tracks with R260 in terms of the UIC classes. It can be seen in Table 1 that the wear is quite different on tracks under different traffic loads. The rails on heavily loaded lines wore at a slower rate as a function of tonnage, with a smaller standard deviation, while those on less loaded lines wore at a quicker rate, with a larger standard deviation. Usually, rail wear happens because of three main reasons: traffic loads, natural corrosion, and grinding. The data in Table 1 does not include grinding effects. Therefore, the reason behind the faster wear rate on less loaded lines is probably because of natural corrosion. Less loaded tracks have more time per tonnage for corrosion. The effect of natural corrosion is considerable because a factor of 12.7 is observed: on UIC-Class 6 it was 4.2 mm/100MGT, whereas on UIC-Class 3, it was 0.33 mm/100MGT. UIC-Class 4 tracks had a wear rate that is nearest to that of [20].

Figure 5 shows the vertical wear rate with respect to track radius and UIC class.

In Figure 5, the horizontal axis is the track radius,  $R_i = 1, 2, \dots, 9$  as defined in (2), and the vertical axis is the vertical wear rate (high rail in curves and average of both rails in straight tracks). The wear rate in logarithm is a linear function of the radius, i.e.,

$$\lg(y_{UICj}) = k \cdot R_i + \lg(y_0) \quad (4)$$

where  $y_0$  is the vertical wear extrapolated to radius = 0; they are 0.554, 0.926, 2.115 and 6.117 for UIC $j$ ,  $j = 3, 4, 5$  and 6, respectively.

Note that (4) is equivalent to

$$y_{UICj} = y_0 \cdot 10^{k \cdot R_i} \quad (5)$$

The four curves in Figure 5 are approximately parallel to each other, meaning that in (4) they have approximately the same  $k$  value. This  $k$  equals  $-0.025$ .

Thus, the vertical wear rate in mm/100 MGT of R260 is, on the Belgium network, as a function of curve radius and traffic load, including corrosion:

$$y_{R260\_2012\_vertical\ wear} = y_0(j) \cdot 10^{-0.025R_i}, \quad R_i = 1, 2, \dots, 9 \text{ and } j \in \{3, 4, 5, 6\} \quad (6)$$

with  $y_0(j) = 0.55, 0.93, 2.12$  and  $6.11$  for  $j = 3, 4, 5, 6$ , respectively.



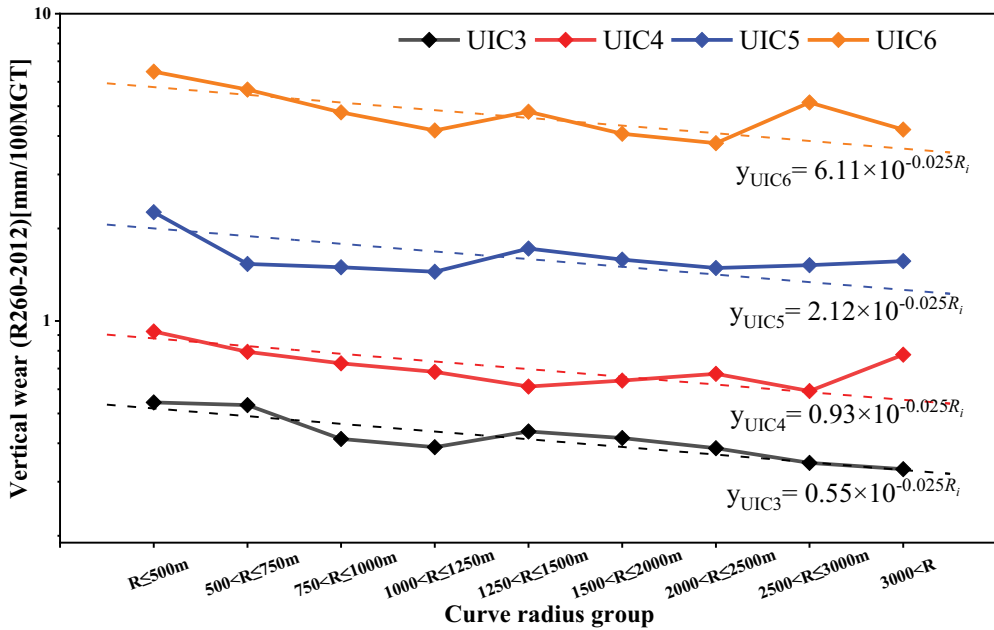


**Figure 5.** Vertical wear of high rail with R260 in 2012 in relation to UIC class and curve radius. (wears of high and low rails are averaged at each tangent track, i.e.  $R > 3000\text{m}$ ; the R-Squared values of the fittings for UIC3, UIC4, UIC5 and UIC6 are 0.784, 0.343, 0.240 and 0.453, respectively).

### 3.2. 45° wear versus tonnage of rails with R260 in 2012

With a decrease in the curve radius, the rail-wheel contact at the high rail shifts towards the gauge corner. The narrower the curve is, the more pronounced this phenomenon will be. Wear in curves is therefore characterized by wear at an angle of 45°. Figure 5 shows the wear at 45° for all radius groups. The logarithmic wear rate roughly linearly increased with decreasing curve radius. The influence of the daily load of the track is important, similar to the vertical wear rate in Section 3.1. The lower the daily tonnage was, the faster the wear per tonnage. In narrow curves with a radius of less than 500 m, the wear evolves on average two to three times as fast as in a tangent section of the track; the wear rate of UIC3 is, for example, 0.4 for  $R > 3000$  and 0.96 for  $R < 500$  m in Figure 6. Also, Figure 6 shows a high wear rate with low tonnage due to corrosion.

Following the same way of deriving (4) – (6), the 45° wear rate rail in mm/100MGT of an R260 high rail is, on the Belgium network, as a function of curve radius and traffic load, including corrosion:

$$Y_{R260\_2012\_45^\circ \text{ wear}} = y_0(j) \cdot 10^{-0.042R_i}, \quad R_i = 1, 2, \dots, 9 \text{ and } j \in \{3, 4, 5, 6\} \quad (7)$$

with  $y_0(j) = 0.95, 1.42, 4.06$  and  $9.38$  for  $j = 3, 4, 5, 6$ , respectively.

### 3.3. Wear versus tonnage for R200 and R260 in 2012

#### 3.3.1. Vertical wear at tangent tracks

The 2012 wear rates of R200 and R260 are compared in Table 2.

On average, the R200 rail will wear 34% faster than the R260 rail in a tangent section of the track. Low tonnage lines show high wear rates per tonnage, which is the effect of corrosion. The wear rate is higher for the R200 steel grade compared to R260. UIC4 seems to be the load with which the 2 grades behave the most similarly, considering the effect of corrosion.

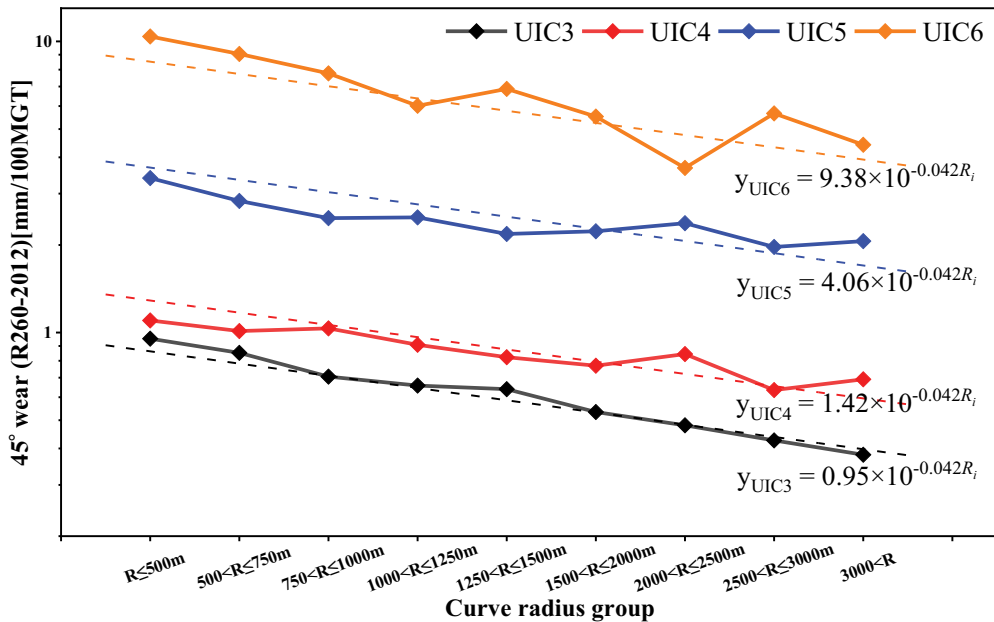


**Figure 6.** 45° wear of high rail with R260 in 2012 in relation to UIC-class and curve radius. (wears of high and low rails are averaged at each tangent track, i.e.  $R > 3000\text{m}$ ; the R-Squared values of the fittings for UIC3, UIC4, UIC5 and UIC6 are 0.968, 0.892, 0.755 and 0.811, respectively).

**Table 2.** Comparison between R200 and R260 in terms of vertical wear at tangent tracks in 2012.

UIC-Class	Vertical wear [mm/100MGT]		Difference
	R260	R200	
UIC3	0.33	0.44	33%
UIC4	0.78	0.80	3%
UIC5	1.57	1.93	23%
UIC6	4.20	9.94	137%
<b>Average*</b>	<b>0.95</b>	<b>1.27</b>	<b>34%</b>

\* The average is calculated based on the kilometres in each UIC class in Table 1.

### 3.3.2. 45° wear at curves

Most of the R200 rails are present in the low-loaded lines, as these are also the oldest rails. Thus, UIC6 is chosen for comparison in Figures 7 and 8. Figure 7 shows the wear at 45° in the curves for R200 and R260 in 2012.

As shown in Figure 7, there is an approximate constant difference, with a scale of about 1.93, between the wear rates of R200 and R260, i.e., the wear rate of R200 is proportional to and 1.93 times as high as that of R260. The average difference between R200 and R260 at 45° is comparable with the literature, i.e., R260 has 34% less wear (Table 2) [21].

Figure 8 shows the comparison between 2012 and 2019 in terms of 45° wear of high rail for UIC6 in relation to the curve radius for R200.

A deviation is nevertheless noted in Figures 7 and 8 for  $R \leq 500\text{m}$ . The wear seems to be much less than expected for R200 in curves with a radius of less than 500 m. A more detailed analysis attributes this deviation to the technical inventory not being updated. Due to the high wear rates, the high rail was more frequently replaced, sometimes without updating the technical inventory.

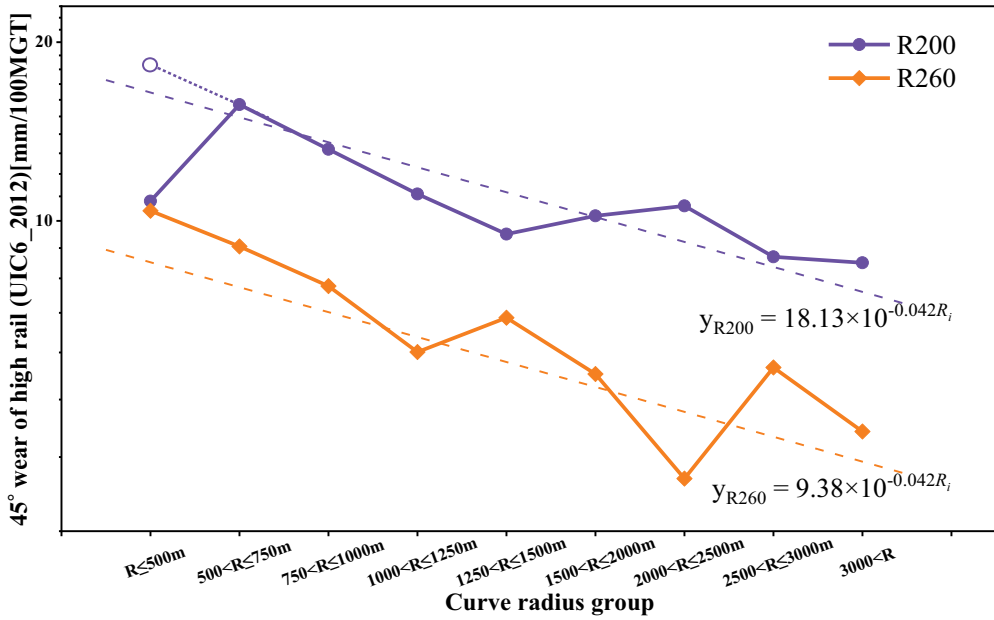


Figure 7. 45° wear of high rail with R200 or R260 in 2012 for UIC6 in relation to curve radius (the R-Squared values of the fittings for R200 and R260 are 0.529 and 0.811, respectively).

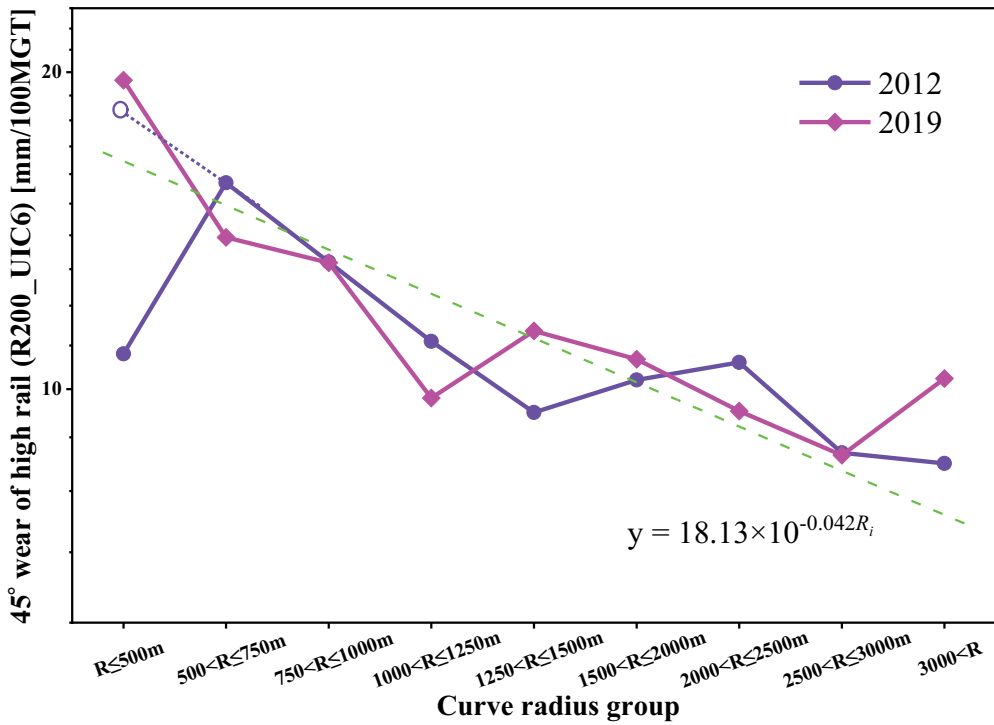


Figure 8. 45° wear of high rail with R200 in 2012 and 2019 for UIC6 in relation to curve radius (the R-Squared values of the fittings for 2012 and 2019 are 0.529 and 0.658, respectively).

This inconsistency is not observed with either R260 in 2012 (Figure 7) or R200 in 2019 (Figure 8), because there has been much emphasis on keeping the technical inventory data up to date in recent years. The 2019 measurements are more consistent in the curves with a small radius (Figure 8). If extrapolating the 2012 R200 wear rate to a radius of less than 500 m, as indicated by the dotted line in Figures 7 and 8, it can be seen in Figure 8 that the wear rate of R200 has a good agreement between 2012 and 2019.

### 3.4. Influence of preventive grinding

Since 2012, Infrabel has introduced a preventive maintenance strategy in which the rails are periodically ground to remove shallow cracks in the rail surface. This strategy should influence rail wear because grinding creates artificial wear. The wear data from 2012 and 2019 are compared to investigate whether this preventive maintenance is visible in the data.

For the R200 rails, there should be no pronounced difference in the wear rate between 2012 and 2019 because the preventive grinding strategy focuses on recently installed rails on important, high-loaded lines. Usually, these lines are equipped with R260, installed after 1982. Between 2012 (the start of the preventive grinding strategy) and 2018, a total of 10.536 km of tracks were ground with two or more grinding passes.

Figure 9 shows that in tangent tracks, the wear of R260 was higher in 2019 than in 2012 due to preventive grinding, except for UIC class 4. For UIC4, the wear in 2012 and 2019 are equal, meaning there was a lack of grinding for UIC4 tracks, assuming that the mechanical wear rate due to wheel-rail contact is the same, as was argued in Section 3.3.2.

Figure 10 shows that the wear in R200 was equal in 2019 and 2012. This can be explained by the fact that the preventive grinding campaigns were focused on recent rails (R260). Figure 10 shows the curves overlay with each other almost perfectly, indicating a very good consistency and, thus, reliability of the measurement data. Since this consistency is observed in the entire network for each load class (UIC3, 4, 5, 6) (Figure 10) and each radius group (Figure 8), it is reasonable to believe that the other data shown in this paper are also consistent and reliable, as they are collected in the same way on the same network in the same period.

In 2019, the wear rate of R260 rails in tangent tracks was higher than that of R200 due to preventive grinding (compare Figures 9 and 10). Taking the R260 natural wear rates of 2012 and 2019 being

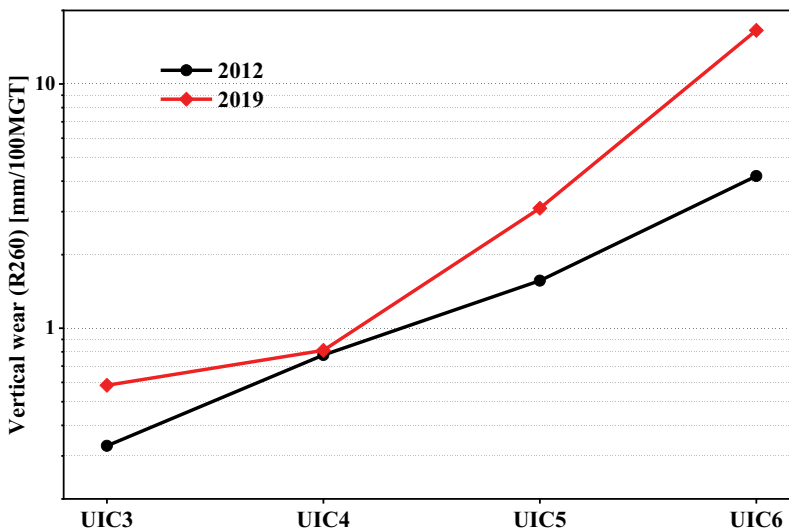


Figure 9. Vertical wear at tangent tracks (average of high and low rails) in 2012 and 2019 for R260.

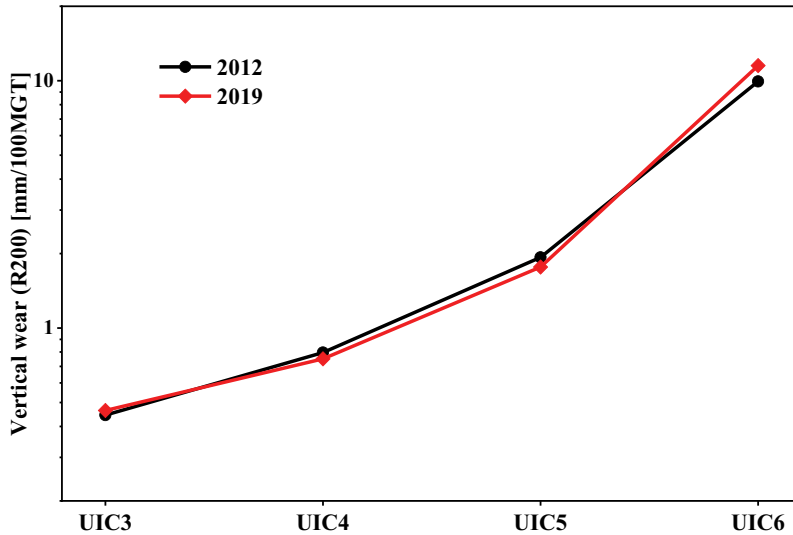


Figure 10. Vertical wear at tangent tracks (average of high and low rails) in 2012 and 2019 for R200.

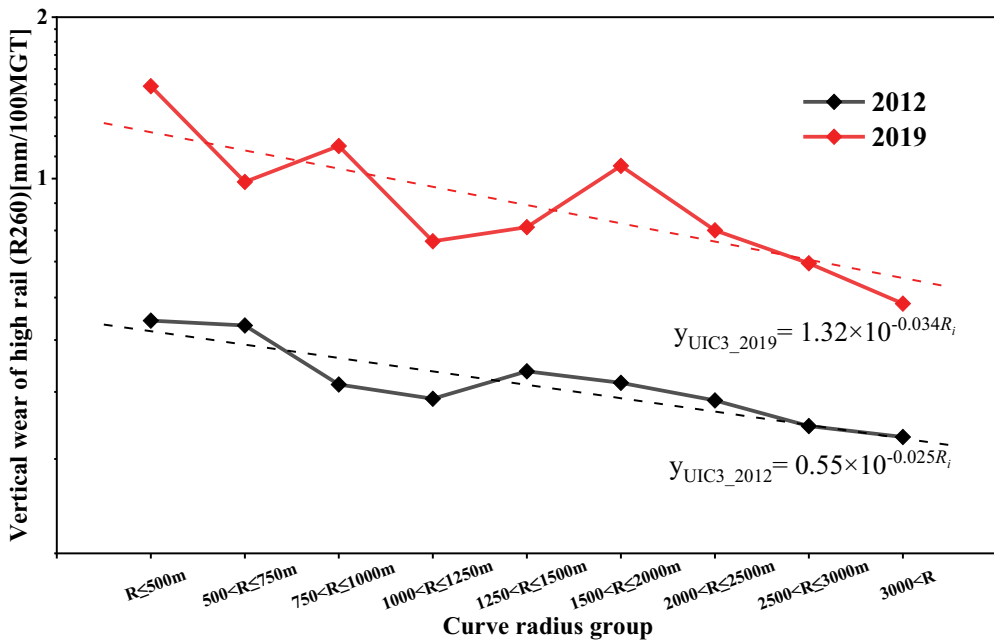


Figure 11. Vertical wear (high rail in curves and average both rails in straight track) in mm/MGT in relation to curve radius – comparison of 2012 and 2019 (R260 – UIC3) (the R-Squared values of the fittings for 2012 and 2019 are 0.787 and 0.652, respectively).

equal, the artificial wear can be calculated. With UIC3 in Figure 9, the mechanical and natural wear was 0.33 mm/100MGT, and the artificial vertical wear was 0.25 mm/100MGT on average between 2012 and 2019 for tangent tracks (i.e.,  $R > 3000$  m). The artificial wear combined with the natural wear made the total wear of R260 higher than the total wear of R200, which was natural wear only.

The difference between 2012 and 2019 is even more pronounced in the curves, as shown in Figure 11 below, taking UIC3 as an example. The artificial wear in curves is higher

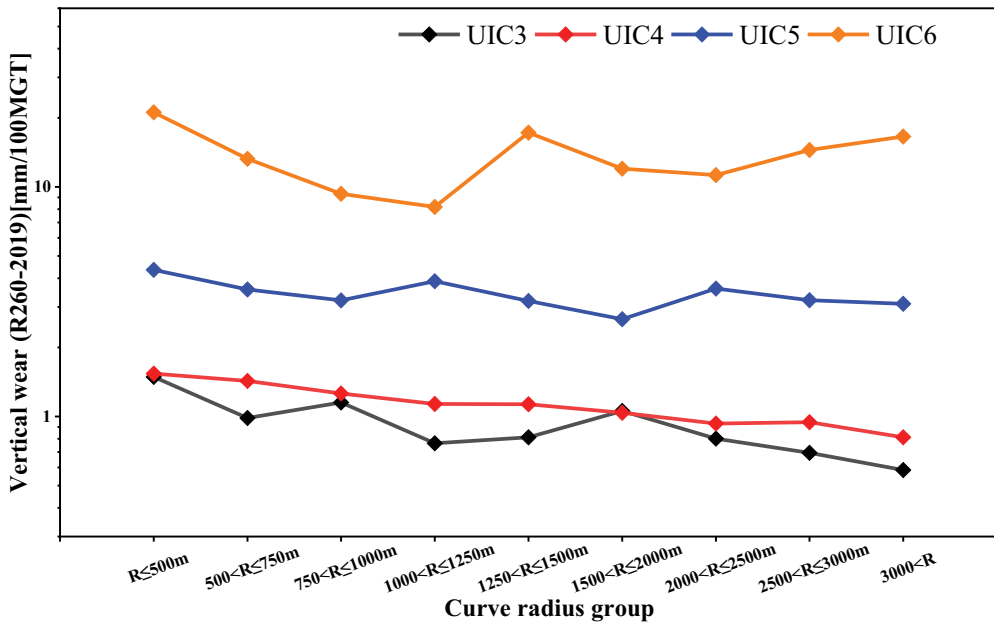


Figure 12. Vertical wear (high rail in curves and average both rails in straight track) in relation to curve radius in 2019 (R260).

compared with tangent tracks mainly because curves need more preventive maintenance. Between 2012 and 2016, the grinding interval was 80 MGT for both curved and tangent tracks. Since 2016, the grinding interval is 25 MGT in curves and 60 MGT in tangent tracks.

Figure 12 shows the average vertical wear rates of 2019 for the 4 UIC load classes.

Comparing Figures 12 with 5, all the measurements show higher wear rates in 2019 than in 2012 due to the preventive grinding. Figure 12 also shows that the UIC4 curve almost overlaps with that of UIC3, meaning that the UIC4 rail had the least grinding, in line with what can be seen in Figure 9.

### 3.5. Vertical wear per year

In previous analyses, wear was expressed in mm/100MGT. In this section, wear will be expressed in mm/year since the installation of the rails, calculated as follows:

$$\Delta w_{vertical}^{yearly} = \frac{w_t}{t - t_0} \quad (8)$$

where  $\Delta w_{vertical}^{yearly}$  is the wear rate per year in mm/year measured in year  $t$ ,  $w_t$  [mm] is the wear measured in year  $t$ , and  $t_0$  is the year of the rail installation.

Figure 13 shows the vertical wear per UIC group in relation to the curve radius based on the measurements performed in 2012.

The wear increased when the curve radius was narrower. The wear rate per year also increased when the daily load was increased, contrasting the trend of the wear rate per tonnage. A higher daily load produces more wear per year. Corrosion is time-related and most likely causes fewer differences between the UIC classes compared with the analysis in mm/100MGT, where the influence of time is less important. Steel without any protection will corrode under atmospheric conditions, and time becomes an important parameter for the lower tonnage tracks.

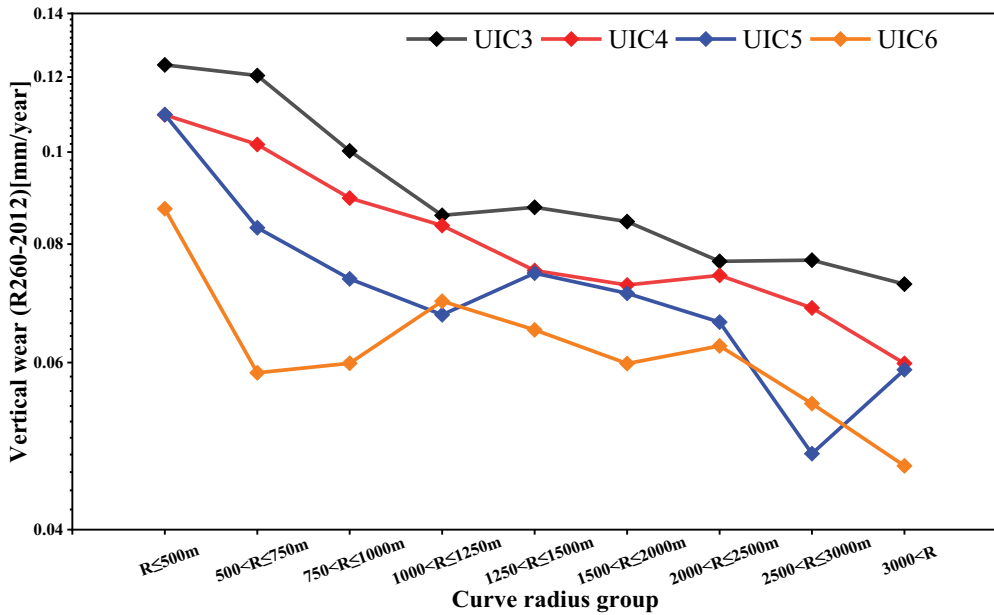


Figure 13. Vertical wear rate in mm/year in relation to UIC class and curve radius in 2012 (R260).

#### 4. Conclusions

Rail wear rate of the whole Belgian network from two measuring campaigns (2012–4,409 km and 2019–5,338 km) has been calculated and analysed. The effects on the wear rate of the curve radius, steel grade, UIC class, and grinding influence has been assessed and discussed. The following conclusions are drawn:

- (1) for both vertical wear and  $45^\circ$  wear, the rail wear rate (mm/100MGT) in the logarithm scale is found to be an approximately linear function of curve radius. The gradient can be considered the same for different UIC classes.
- (2) the wear rate for rails with grade R200 is proportional to and 1.93 times as high as that for rails with grade R260.
- (3) the artificial wear due to rail grinding makes the rail wear rate not a linear function of curve radius in the logarithm scale (as is the case for natural wear. Comparing the wear data between 2012 and 2019, the effect of the preventive grinding strategy in Belgium is clearly shown.
- (4) when the rail wear rate is calculated in mm/100MGT, the rail wear shows to be much faster in less busy traffic lines. However, when the rail wear rate is calculated in mm/year, the higher the tonnage, the higher the rail wear rate. Wear rate analyses are recommended per UIC class, thus for better-guided maintenance.
- (5) the rail wear rates do not show significant variations with changes in rolling stock over the years, which implies that the estimated wear rates in this paper could also possibly hold for other networks.

There are still gaps in the current knowledge of rail steel wear data and wear mechanisms. For example, in further research, the role of corrosion in low-loaded lines is to be quantified and analysed, including its influences on wear and its possible consequences on rolling contact fatigue. Further research can also be done to derive the wear laws for each point of the rail profile by simulating the wear process of the Belgium railway network [22]. Such simulation can

be done with vehicle dynamic modelling considering detailed wheel-rail contact solution [3]. The wear can be assumed to be proportional to the local frictional work in the contact patch [3,23]. The simulated worn profile should match the measured profiles. Such wear laws can then be used for predicting the evolution of the rail profiles and for optimizing monitoring and maintenance procedures of rail [24]. Many railway networks have rolled out a preventive grinding strategy in recent decades. The magic wear rate needed to control preventive maintenance depends on the annual tonnage. Further research on how RCF evolves (mm/ton and mm/year) in lines with different annual tonnages, including the findings on wear behaviour obtained in this paper, is needed.

## Disclosure statement

No potential conflict of interest was reported by the author(s).

## ORCID

Li Wang  <http://orcid.org/0000-0001-7244-803X>

## References

- [1] Krause H, Poll G. Wear of wheel-rail surfaces. *Wear*. 1986;113(1):103–122. doi: 10.1016/0043-1648(86)90060-8
- [2] Zoeteman A, Dollevoet R, Li Z. Dutch research results on wheel/rail interface management: 2001-2013 and beyond. *Proc Inst Mech Eng F J Rail Rapid Transit*. 2014;228(6):642–651. doi: 10.1177/0954409714524379
- [3] Li Z. Wheel-rail rolling contact and its application to wear simulation. PhD thesis, Delft University of Technology, 2002.
- [4] Li Z, Kalker J. Simulation of severe wheel-rail wear. *Trans Built Environ*. 1998;34:393–402.
- [5] Enblom R, Berg M. Proposed procedure and trial simulation of rail profile evolution due to uniform wear. *Proc Inst Mech Eng F J Rail Rapid Transit*. 2008;222(1):15–25. doi: 10.1243/09544097JRR173
- [6] Ranjha S, Mutton P, Kapoor A. Effect of head wear and lateral forces on underhead radius crack propagation. *Proc Inst Mech Eng F J Rail Rapid Transit*. 2014;228(6):620–630. doi: 10.1177/0954409714537251
- [7] Christoforou P, Fletcher D, Lewis R. Benchmarking of premium rail material wear. *Wear*. 2019;436-437:202990. doi: 10.1016/j.wear.2019.202990
- [8] Lewis R, Olofsson U. Mapping rail wear regimes and transitions. *Wear*. 2004;257(7–8):721–729. doi: 10.1016/j.wear.2004.03.019
- [9] Olofsson U, Nilsson R. Surface cracks and wear of rail: a full-scale test on a commuter train track. *Proc Inst Mech Eng F J Rail Rapid Transit*. 2002;216(4):249–264. doi: 10.1243/095440902321029208
- [10] Olofsson U, Terriskivi T. Wear, plastic deformation and friction of two rail steels—a full-scale test and a laboratory study. *Wear*. 2003;254(1–2):80–93. doi: 10.1016/S0043-1648(02)00291-0
- [11] Li W, Wang P, Wang S, et al. Wheel-rail wear simulation and rail cant optimization based on railway vehicle dynamics. *Int J Veh Perform*. 2021;7(1–2):4–20. doi: 10.1504/IJVP.2021.113410
- [12] Chang C, Wang C, Chen B, et al. A study of a numerical analysis method for the wheel-rail wear of a heavy haul train. *Proc Inst Mech Eng F J Rail Rapid Transit*. 2010;224(5):473–482. doi: 10.1243/09544097JRR1341
- [13] Ignesti M, Malvezzi M, Marini L, et al. Development of a wear model for the prediction of wheel and rail profile evolution in railway systems. *Wear*. 2012;284–285:1–17. doi: 10.1016/j.wear.2012.01.020
- [14] Innocenti A, Marini L, Meli E, et al. Development of a wear model for the analysis of complex railway networks. *Wear*. 2014;309(1):174–191. doi: 10.1016/j.wear.2013.11.010
- [15] Butini E, Marini L, Meacci M, et al. An innovative model for the prediction of wheel-rail wear and rolling contact fatigue. *Wear*. 2019;436–437:203025. doi: 10.1016/j.wear.2019.203025
- [16] Wang H, Wang W, Han Z, et al. Wear and rolling contact fatigue competition mechanism of different types of rail steels under various slip ratios. *Wear*. 2023;522:204721. doi: 10.1016/j.wear.2023.204721
- [17] EN13674-1. Railway applications - track - rail part 1: vignole railway rails 46 kg/m and above. 2011.
- [18] Wei K, Chen R, Xu Y. Rail profile wear on curve and its effect on wheel-rail contact geometry. *Adv Mater Res*. 2013;779-780:655–659. doi: 10.4028/www.scientific.net/AMR.779-780.655
- [19] UIC (International Union of Railways). Classification of lines for the purpose of track maintenance. Paris: Leaflet 714 R, International Union of Railways; 1989.
- [20] Lichtberger B. Track compendium: track system, substructure, maintenance, economics. Hamburg: DVV Media Group GmbH Eurailpress; 2011.



- [21] Stock R, Pippan R. RCF and wear in theory and practice—the influence of rail grade on wear and RCF. *Wear*. 2011;471(1–2):125–133. doi: [10.1016/j.wear.2010.10.015](https://doi.org/10.1016/j.wear.2010.10.015)
- [22] Zobory I. Prediction of wheel/rail profile wear. *Veh Syst Dyn*. 1997;28(2–3):221–259. doi: [10.1080/00423119708969355](https://doi.org/10.1080/00423119708969355)
- [23] Ignesti M, Innocenti A, Marini L, et al. Development of a wear model for the wheel profile optimization on railway vehicles. *Veh Syst Dyn*. 2013;51(9):1363–1402. doi: [10.1080/00423114.2013.802096](https://doi.org/10.1080/00423114.2013.802096)
- [24] Bosso N, Magelli M, Zampieri N. Simulation of wheel and rail profile wear: a review of numerical models. *Rail Eng Sci*. 2022;30(4):403–436. doi: [10.1007/s40534-022-00279-w](https://doi.org/10.1007/s40534-022-00279-w)